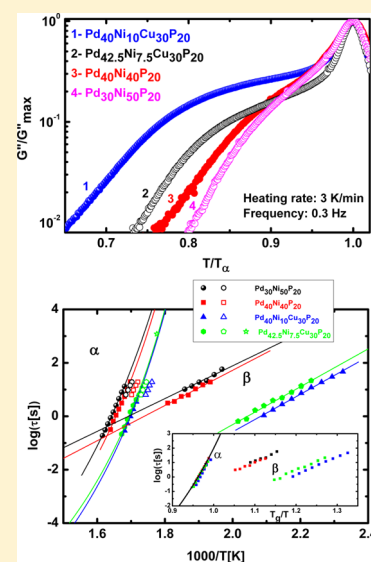


## Characteristics of the Structural and Johari–Goldstein Relaxations in Pd-Based Metallic Glass-Forming Liquids

Jichao Qiao,<sup>†</sup> Riccardo Casalini,<sup>‡</sup> Jean-Marc Pelletier,<sup>\*,†</sup> and Hidemi Kato<sup>§</sup><sup>†</sup>Université de Lyon, MATEIS, UMR CNRS5510, Bat. B. Pascal, INSA-Lyon, F-69621 Villeurbanne cedex, France<sup>‡</sup>Chemistry Division, Naval Research Laboratory, Code 6120, Washington, DC 20375-5342, United States<sup>§</sup>Institute for Materials Research, Tohoku University, Sendai, Miyagi 980-8577, Japan

**ABSTRACT:** The dynamics of Pd-based metallic glass-forming liquids ( $\text{Pd}_{40}\text{Ni}_{10}\text{Cu}_{30}\text{P}_{20}$ ,  $\text{Pd}_{42.5}\text{Ni}_{7.5}\text{Cu}_{30}\text{P}_{20}$ ,  $\text{Pd}_{40}\text{Ni}_{40}\text{P}_{20}$ , and  $\text{Pd}_{30}\text{Ni}_{50}\text{P}_{20}$ ) was studied by mechanical spectroscopy and modulated differential scanning calorimetry (MDSC). We found that the change in composition has a significant effect on the  $\alpha$  relaxation dynamics; the largest difference corresponds to an increase of the glass transition temperature  $T_g$  of  $\sim 15$  K, for materials in which 30% Ni was substituted by 30% Cu (i.e., from  $\text{Pd}_{40}\text{Ni}_{40}\text{P}_{20}$  to  $\text{Pd}_{40}\text{Ni}_{10}\text{Cu}_{30}\text{P}_{20}$ ). We also found that all Pd-based metallic glasses have very similar fragilities,  $59 < m < 67$ , and Kohlrausch stretched exponents,  $0.59 < \beta_{\text{KWW}} < 0.60$ . It is interesting that the values of  $m$  and  $\beta_{\text{KWW}}$  correlate well with the general relation proposed by Böhmer et al. for nonmetallic glass formers (Böhmer, R.; et al. *J. Chem. Phys.* **1993**, *99*, 4201–4209), which for the observed  $\beta_{\text{KWW}}$  values predicts  $58 < m < 61$ . From a linear deconvolution of the  $\alpha$  and  $\beta$  relaxations, we find that the substitution of the Ni with Cu induced a large change in the time constant of the Johari–Goldstein relaxation,  $\tau_\beta$ . The activation energy,  $U_\beta$ , of the  $\beta$  relaxation was largely independent of chemical composition. In all cases,  $25 < U_\beta/RT < 28$ , a range in agreement with results for other glass formers (Kudlik, A.; et al. *Europhys. Lett.* **1997**, *40*, 649–654 and Ngai, K. L.; et al. *Phys. Rev. E* **2004**, *69*, 031501). From the heat capacity and mechanical loss, estimates were obtained for the number of dynamically correlated units,  $N_c$ ; we find significantly larger values for these metallic glass-forming liquids than  $N_c$  for other glass-forming materials.



## 1. INTRODUCTION

One of the most intriguing issues in supercooled liquids and glassy materials is their dynamic relaxation behaviors, which underlies their physical and mechanical properties.<sup>1–3</sup> Mechanical relaxation in amorphous materials depends on the chemical structure and the morphology. Typical mechanical or dielectric relaxation spectra show two relaxation processes in amorphous materials.<sup>4–7</sup> The primary (or  $\alpha$ ) relaxation corresponds to structural relaxation, which is coupled to molecular diffusion. The  $\alpha$  relaxation time,  $\tau_\omega$  increases by many orders of magnitude on cooling from the liquid to the glassy state. In amorphous metallic alloys, the  $\alpha$  relaxation has been extensively investigated by differential scanning calorimetry (DSC),<sup>8–10</sup> density relaxation,<sup>11,12</sup> viscosity,<sup>13</sup> free volume changes,<sup>14</sup> dynamic mechanical relaxation,<sup>15–18</sup> and positron annihilation spectroscopy.<sup>19</sup> For metallic glass formers, the  $\alpha$  relaxation is ascribed to the cooperative motion of atoms.<sup>1,5</sup> The temperature dependence of  $\tau_\alpha$  invariably conforms to the Vogel–Fulcher–Tamman (VFT) equation.<sup>20</sup> A second faster relaxation, usually evident only below the glass transition temperature  $T_g$ , is known as the Johari–Goldstein (JG) relaxation, a type of secondary (or  $\beta$ ) relaxation related to more local dynamics.<sup>4,20–22</sup> The  $\alpha$  and  $\beta$  relaxations both appear to be universal features of amorphous materials. The relationship between the two processes, and in particular

whether the  $\beta$  functions as the precursor to structural relaxation, is a topic of current debate.<sup>5</sup> In metallic glasses, there exist “liquid-like sites” embedded in an elastic matrix.<sup>1</sup> These liquid-like sites (or regions) are thought to be related to both the secondary relaxation and plastic deformation.<sup>23</sup> The dynamics of metallic glass-forming liquids is more complicated than for molecular liquids, since the former show an additional fragile-to-strong dynamic transition.<sup>24</sup>

Calorimetry is a useful method to investigate the  $\alpha$  and  $\beta$  relaxations in glass-forming materials.<sup>25–27</sup> From such measurements, Hu et al. found a correlation in metallic glasses between the activation energy of the  $\beta$  relaxations  $U_\beta$  and  $T_g$ ,  $U_\beta = 26.1 RT_g$ .<sup>25</sup> They concluded that the Johari–Goldstein relaxation is an intrinsic feature of amorphous metallic alloys. This empirical correlation between  $U_\beta$  and  $T_g$  was confirmed by Yang et al.<sup>19</sup> in isothermally annealed  $\text{Al}_{85}\text{Ni}_5\text{Y}_8\text{Co}_2$  and  $\text{Al}_{85}\text{Y}_5\text{Y}_6\text{Co}_2\text{Fe}_2$ . Interestingly, Haruyama et al.<sup>11</sup> showed the  $\beta$  relaxation in  $\text{Zr}_{55}\text{Cu}_{30}\text{Ni}_5\text{Al}_{10}$  metallic glass is mainly attributed to chemical short-range ordering (CSRO).

Okumura et al.<sup>28–30</sup> observed the  $\beta$  relaxation in La-based metallic glass by dynamic mechanical analysis (DMA).

Received: December 12, 2013

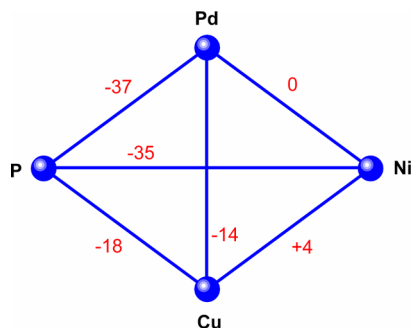
Revised: March 10, 2014

Published: March 10, 2014

Substitution of Cu with Ni in  $\text{La}_{35}\text{Al}_{25}\text{Ni}_{20}$  metallic glass caused the  $\beta$  relaxation to be suppressed, appearing as an excess wing.<sup>28</sup> An opposite result has been reported by Wang et al.<sup>31</sup> The nonequilibrium and inherently unstable nature of glassy materials is affected by physical aging.<sup>32–35</sup> In turn, the aging dynamics is related to the structural relaxation process.<sup>34,35</sup> Pelletier et al.<sup>36</sup> reported the existence of a  $\beta$  relaxation at low temperature in  $\text{Pd}_{43}\text{Ni}_{10}\text{Cu}_{27}\text{P}_{20}$  metallic glass by mechanical spectroscopy, which they ascribed to the nonmetallic elements (i.e., P) surrounding the metallic-bonding regions. Using ultrasonic annealing of the Pd–Ni–Cu–P, Ichitsubo et al. showed that the microstructural patterns consisted of strongly bonded regions (SBRs) surrounded by weakly bonded regions (WBRs).<sup>37,38</sup> It has been pointed out that, in glassy alloys, SBRs have a high shear modulus and low Poisson ratio, while WBRs have a low shear modulus and high Poisson ratio. The authors inferred that the  $\beta$  relaxation of Pd-based metallic glass is connected to the WBRs, being related to the inhomogeneous microstructure.<sup>37,38</sup> The heterogeneous structure on the nanoscale in metallic glass-forming liquids has also been observed by high resolution transmission electron microscopy (HRTEM),<sup>39–41</sup> by dynamic atomic force microscopy,<sup>42</sup> and in simulations.<sup>43,44</sup> These results suggest that the nanoscale heterogeneities in amorphous metallic alloys are connected to the  $\beta$  relaxation.

Generally, the mechanical behavior, physical properties, and relaxation behaviors are strongly dependent on the nature of the constituent atoms or molecules.<sup>6,45</sup> In the current investigation, mechanical tests using DMA and temperature modulated differential scanning calorimetry (MDSC) were performed to probe the characteristics of the Johari–Goldstein relaxations in Pd-based metallic glass-forming liquids, in particular, the influence of minor changes in the chemical content on the JG process. Recently, Yu et al.<sup>6</sup> found that the  $\beta$  relaxations in metallic glass-forming liquids are sensitive to the chemical interactions among all the constituent atoms. In other words,  $\beta$  relaxations in metallic glasses are linked to a large mixing enthalpy for the atoms.<sup>6</sup> The enthalpy of mixing among all the constituent atoms in Pd–Ni–Cu–Al is reported in Scheme 1. In the previous work, it was proposed that the  $\beta$  relaxation is enhanced by replacing Ni by Cu atoms.<sup>6</sup> Applying the time–temperature superposition (TTS) principle, we show that the activation energies of the JG relaxations are comparable to those of other glass-forming materials. We find that the JG relaxation is suppressed with increasing concentration of Ni, in

**Scheme 1. The Schematics of Enthalpy of the Mixing Elements for the Pd–Ni–Cu–P System Metallic Glass-Forming Liquids<sup>a</sup>**



<sup>a</sup>The values of the enthalpy of mixing come from ref 6.

agreement with previous observations.<sup>6</sup> Finally, the number of correlating units was determined using two different approaches. We found that the number of correlating units is significantly larger than that in other glass-forming liquids, which could be interpreted as a reflection of short-range ordering in these metallic glass-forming liquids.

## 2. EXPERIMENTAL PROCEDURE

**2.1. Sample Preparation.** Master alloys of palladium-based bulk metallic glasses were fabricated by the  $\text{B}_2\text{O}_3$  flux method. Metal chips of Pd (99.5%), Ni (99.99%), Cu (99.99%), and lump P (99.9999%) were mixed together and sealed in an evacuated quartz tube, and the mixture compositions were melted under inert argon gas in a resistance heating furnace. In the current work, the compositions of the alloys (atom %) are  $\text{Pd}_{40}\text{Ni}_{10}\text{Cu}_{30}\text{P}_{20}$ ,  $\text{Pd}_{42.5}\text{Ni}_{7.5}\text{Cu}_{30}\text{P}_{20}$ ,  $\text{Pd}_{40}\text{Ni}_{40}\text{P}_{20}$ , and  $\text{Pd}_{30}\text{Ni}_{50}\text{P}_{20}$ , respectively. The experimental details are described as previous literature.<sup>46</sup>

**2.2. Differential Scanning Calorimetry (DSC).** Differential scanning calorimetry (DSC) experiments were performed using a standard commercial instrument (PerkinElmer, DSC-7) under high purity dry nitrogen at a flow rate of 20 mL/min. Aluminum pans were used as sample holders. Baseline corrections during the experiments were made for all the DSC curves. In order to ensure the reliability of the data in the experiments, a temperature calibration was performed prior to conducting the experiments with an indium standard specimen with 6.146 mg ( $T_m = 429.7\text{K}$ ,  $\Delta H_c = 28.48\text{ J/g}$ ) and zinc standard with 3.283 mg ( $T_m = 692.6\text{K}$ ,  $\Delta H_c = 108.37\text{ J/g}$ ), giving an accuracy of  $\pm 0.2\text{ K}$  and  $\pm 0.02\text{ mW}$ , respectively. In order to get better accuracy during the experiments, all the samples were of similar mass.

**2.3. X-ray Diffraction (XRD).** X-ray diffraction (XRD) experiments were conducted at room temperature to examine their amorphous character, using Cu  $K\alpha$  radiation produced by a commercial device (D8, Bruker AXS GmbH, Germany).

**2.4. Dynamic Mechanical Analysis (DMA).** Dynamic mechanical measurements were carried out in an inverted torsion mode using a mechanical spectrometer described by Etienne et al.<sup>47</sup> Experiments were performed using a sinusoidal stress, either at a fixed frequency (ranging from  $10^{-2}$  to 2 Hz) during continuous heating with a constant heating rate or at a given temperature with different frequencies. Experimental samples with dimensions of 30 mm (length)  $\times$  2 mm (width)  $\times$  1 mm (thickness) were prepared using electric discharge machining. All the experiments were performed under a high vacuum atmosphere. A periodic shear stress was applied, and the corresponding strain was measured. Thus, the complex modulus ( $G = G' + iG''$ ) was deduced and then the storage ( $G'$ ) and loss ( $G''$ ) dynamic shear modulus were calculated. The loss factor  $\tan \delta = G''/G'$  was also determined. The strain amplitude was lower than  $10^{-4}$ .

**2.5. Modulated Differential Scanning Calorimetry (MDSC).** Modulate differential scanning calorimetry (MDSC) was performed using a TA Q100 calorimeter. Samples were cooled from above the glass transition at a rate of  $q = 0.5\text{ K/min}$ , with temperature modulation of 1 K and modulation periods of  $T_m = 40, 60, 90,$  and  $120\text{ s}$ .

## 3. RESULTS AND DISCUSSION

**3.1. Thermal Properties and XRD Analysis (As-Cast State).** The DSC scans during heating at 20 K/min for the four

investigated Pd-based bulk metallic glasses are presented in Figure 1a. A step corresponding to the glass transition is

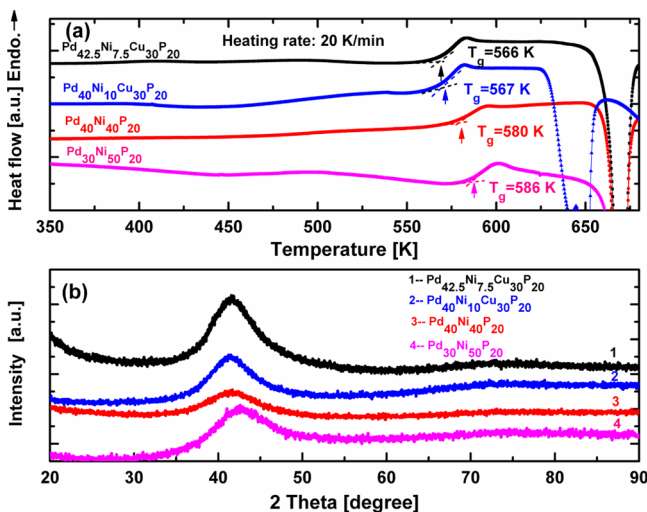


**Figure 1.** (a) DSC curves of the Pd-based bulk metallic glasses (the heating rate is 20 K/min); the glass transition temperatures  $T_g$  are defined by the arrows in the figure. (b) The XRD patterns of the Pd-based metallic glasses in as-cast states. The morphology confirmed the amorphous feature of the Pd-based metallic glasses.

followed by a large exothermic peak related to the crystallization of the sample. The glass transition temperature is found to vary by about 20° depending on the composition, with the alloys containing Cu having a smaller  $T_g$ . The XRD patterns of the four Pd-based metallic glass-forming liquids are reported in Figure 1b; only broad diffraction maxima are observed. The DSC curves and XRD patterns validated the amorphous nature of the model alloys.

**3.2. Evolution of the JG Relaxation in Pd-Based Metallic Glass-Forming Liquids.** **3.2.1. Isochronal Measurements.** Figure 2a shows the temperature dependence of the loss modulus,  $G''/G''_{\max}$ , at constant frequency (0.3 Hz) as a function of temperature for the four investigated Pd-based metallic glass-forming liquids. It is evident that with increasing content of Ni atoms the  $\beta$  relaxation becomes less prominent. For Pd<sub>30</sub>Ni<sub>50</sub>P<sub>20</sub> metallic glass, the  $\beta$  relaxation is present only as a weak shoulder. This is evident also when using the Cole–Cole (CC) representation to describe the overall dynamic mechanical behavior.<sup>48</sup> The CC curves of Pd<sub>40</sub>Ni<sub>10</sub>Cu<sub>30</sub>P<sub>20</sub> and Pd<sub>40</sub>Ni<sub>40</sub>P<sub>20</sub> metallic glass-forming liquids are reported in the inset of Figure 2a; these results are in good agreement with the recent report by Yu et al.<sup>6</sup> Since in their glassy state Pd<sub>30</sub>Ni<sub>50</sub>P<sub>20</sub> has a higher density than Pd<sub>40</sub>Ni<sub>10</sub>Cu<sub>30</sub>P<sub>20</sub>, this dependence of the  $\beta$  relaxation on the composition suggests that this process could be related to local motions of atoms in a less dense part of the material, i.e., a local free volume. Moreover, as observed in ref 6, it is clear from the enthalpy of mixing in Pd-based metallic glass-forming liquids reported in Scheme 1 that the more pronounced  $\beta$  relaxations in Pd<sub>40</sub>Ni<sub>10</sub>Cu<sub>30</sub>P<sub>20</sub> and Pd<sub>42.5</sub>Ni<sub>7.5</sub>Cu<sub>30</sub>P<sub>20</sub> are associated to large negative values of the enthalpy of mixing among the constituting atoms.

In order to further illustrate the thermal heat treatment feature of the  $\beta$  relaxation in Pd-based metallic glass-forming liquids, dynamic mechanical tests were conducted for heated sample Pd<sub>40</sub>Ni<sub>10</sub>Cu<sub>30</sub>P<sub>20</sub> metallic glass (the sample was heated to 590 K with a heating rate of 3 K/min and kept at 590 K for 3

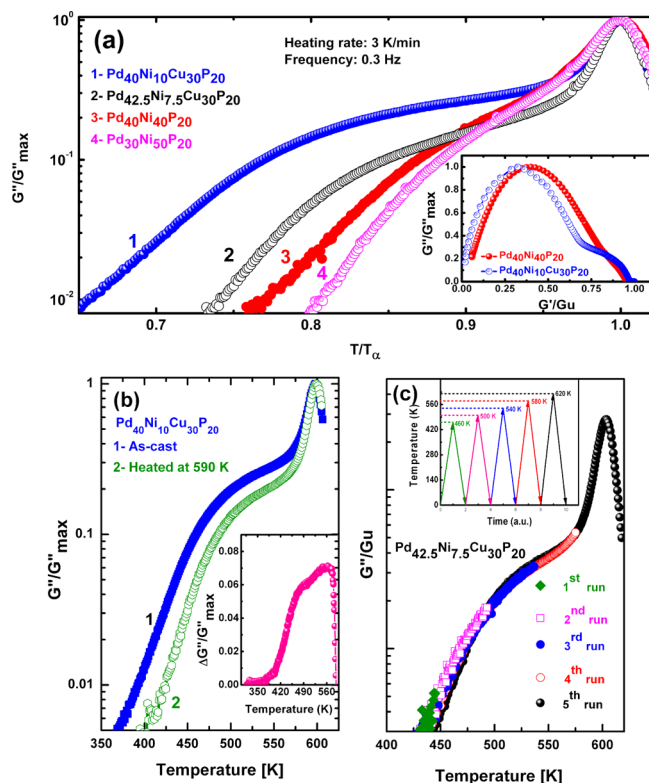


**Figure 2.** (a) Temperature dependence of the loss modulus  $G''/G''_{\max}$  ( $G''_{\max}$  corresponds to the peak of  $\alpha$  relaxation in the loss modulus) in Pd-based metallic glass-forming liquids (heating rate, 3 K/min; driving frequency, 0.3 Hz). The peak temperatures of  $\alpha$  relaxation  $T_{\alpha}$  for Pd<sub>40</sub>Ni<sub>10</sub>Cu<sub>30</sub>P<sub>20</sub>, Pd<sub>42.5</sub>Ni<sub>7.5</sub>Cu<sub>30</sub>P<sub>20</sub>, Pd<sub>40</sub>Ni<sub>40</sub>P<sub>20</sub>, and Pd<sub>30</sub>Ni<sub>50</sub>P<sub>20</sub> are 598, 596, 604, and 615 K, respectively. The evolution of  $T_{\alpha}$  is consistent with those of the DSC results (Figure 1a). The inset shows Cole–Cole plots of the Pd<sub>40</sub>Ni<sub>10</sub>Cu<sub>30</sub>P<sub>20</sub> and Pd<sub>40</sub>Ni<sub>40</sub>P<sub>20</sub> metallic glass-forming liquids. (b) Impact of heat treatment on the  $\beta$  relaxation in Pd<sub>40</sub>Ni<sub>10</sub>Cu<sub>30</sub>P<sub>20</sub> metallic glass (as-cast state and heated the sample to 590 K). The inset shows the variation of  $\Delta G''/G''_{\max}$  ( $\Delta G'' = G''_{\text{as-cast}} - G''_{\text{heated at 590 K}}$ ). The amorphous feature after heat treatment is confirmed by XRD. (c) Evolution of JG secondary relaxation during the successive continuous heating processes for Pd<sub>42.5</sub>Ni<sub>7.5</sub>Cu<sub>30</sub>P<sub>20</sub> metallic glass-forming liquid (heating rate is 3 K/min and driving frequency is 0.3 Hz). The inset presents a schematic illustration of the DMA experiment during the continuous heating process.

min before cooling down at a rate of 10 K/min). The amorphous characteristic of the annealed sample is validated by XRD. A comparison of  $\beta$  relaxation of Pd<sub>40</sub>Ni<sub>10</sub>Cu<sub>30</sub>P<sub>20</sub> metallic glass between the as-cast and after heat treatment is provided in Figure 2b. The heat treatment leads to a reduction in the amplitude of the loss modulus, i.e., the heat treatment induces a decrease of the atomic mobility and amplitude of the JG relaxation (inset of Figure 2b) in the amorphous alloy. It is reasonable to expect that the heat treatment causes the metallic glass to evolve toward a higher density state with a consequent reduction of the available local “free volume” available for atomic rearrangement, since the cooling rate after the heat treatment was smaller than that in the as-cast sample. This is consistent with the  $\beta$  relaxations in metallic glasses being related to localized motion of atoms, with the intensity of the JG  $\beta$  relaxations to a great extent linked to the concentration of “defects”. These defects are termed as “free volume”,<sup>49,50</sup> “weak points”,<sup>37,38</sup> “soft zone”,<sup>39</sup> “flow units”,<sup>1,12</sup> “liquid-like sites”,<sup>51,52</sup> and “quasi-point defects” (QPDs).<sup>53–56</sup> Specifically,

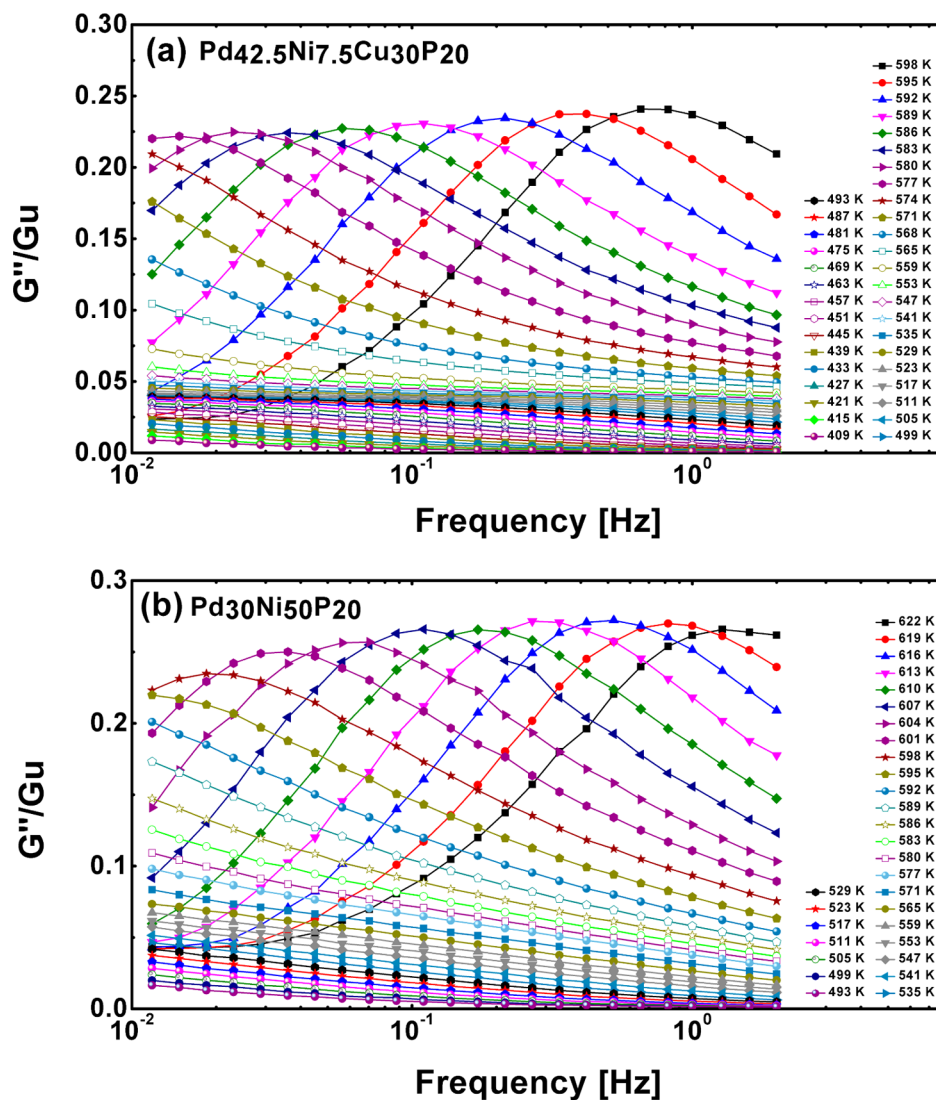


**Figure 3.** The normalized loss modulus spectra  $G''/G_u$  of  $\text{Pd}_{42.5}\text{Ni}_{7.5}\text{Cu}_{30}\text{P}_{20}$  and  $\text{Pd}_{30}\text{Ni}_{50}\text{P}_{20}$  metallic glass-forming liquids as a function of frequency at different temperatures. Parts a and b show the loss modulus spectra of  $\text{Pd}_{42.5}\text{Ni}_{7.5}\text{Cu}_{30}\text{P}_{20}$  and  $\text{Pd}_{30}\text{Ni}_{50}\text{P}_{20}$  metallic glasses, respectively.

these inhomogeneous structures in nano- or microdomain have been confirmed by different techniques or simulation methods.<sup>39–44</sup> A recent review by Yu, Samwer, and Wang examines the mechanical relaxation in metallic glass-forming liquids in detail, in particular the nature of the Johari–Goldstein  $\beta$  relaxation in metallic glasses with different systems.<sup>22</sup> Figure 2c shows the evolution of the  $\beta$  relaxation during the progressive heating process of the  $\text{Pd}_{42.5}\text{Ni}_{7.5}\text{Cu}_{30}\text{P}_{20}$  metallic glass-forming liquid. As expected, for annealing below the glass transition temperature  $T_g$ , we found that the  $\beta$  relaxation is not sensitive to the different heat treatments. This reversibility of the  $\beta$  relation is consistent with the local noncooperative nature of the motion of the atoms related to  $\beta$  relaxation. Due to the local nature of this motion, it is reasonable to expect that it can cause only minor changes to the structure of the glass (Figure 2c).

**3.2.2. Relaxation Processes and the Master Curves.** To study the influence of the frequency on the mechanical relaxation in Pd-based metallic glass-forming liquids, the isothermal spectra of  $G'$  and  $G''$  have been measured. Figure 3 presents the frequency dependence of the loss modulus  $G''$  at various temperatures of  $\text{Pd}_{42.5}\text{Ni}_{7.5}\text{Cu}_{30}\text{P}_{20}$  and  $\text{Pd}_{30}\text{Ni}_{50}\text{P}_{20}$

metallic glasses. Below the glass transition temperature  $T_g$ , the loss modulus increases by increasing the isothermal temperature at a given frequency. Above the glass transition temperature, a loss peak associated with the primary  $\alpha$  relaxation is evident in the spectra.

Assuming the validity of the time–temperature superposition (TTS) principle, we constructed the master curve with respect to a reference temperature  $T_r$ . To obtain this master curve, the loss spectra are shifted by the frequency shift factor  $a_T$ <sup>57</sup>

$$\ln a_T = \ln \tau - \ln \tau_r \quad (1)$$

where  $\tau$  and  $\tau_r$  are the relaxation times at temperatures  $T$  and  $T_r$ , respectively. Assuming an activated (i.e., Arrhenius) behavior of the relaxation time  $\tau$ , it follows<sup>57,58</sup>

$$\ln a_T = \frac{U}{R} \left( \frac{1}{T} - \frac{1}{T_r} \right) \quad (2)$$

here,  $R$  is the gas constant and  $U$  is the apparent activation energy for  $\alpha$  and Johari–Goldstein  $\beta$  relaxations.

The master curves of the Pd-based metallic glasses are obtained by the TTS principle, in the case of the Pd<sub>42.5</sub>Ni<sub>7.5</sub>Cu<sub>30</sub>P<sub>20</sub> metallic glass, which is presented in Figure 4.

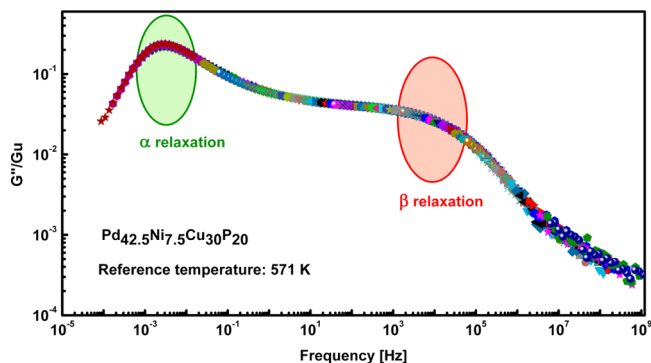


**Figure 4.** Master curves for the loss modulus of Pd<sub>42.5</sub>Ni<sub>7.5</sub>Cu<sub>30</sub>P<sub>20</sub> bulk metallic glass. The reference temperature is 571 K.

At lower frequency, the master curve is dominated by the  $\alpha$  relaxation peak, while, at high frequency, the presence of the Johari–Goldstein  $\beta$  relaxation is evident. A comparison of the master curves in the Pd-based metallic glass-forming liquids is shown in Figure 5. The master curves of these amorphous

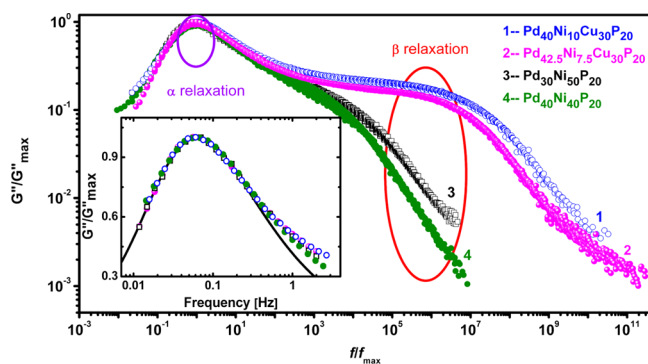


**Figure 5.** Master curves for the loss modulus of Pd-based metallic glass-forming liquids. The reference temperatures of Pd<sub>40</sub>Ni<sub>10</sub>Cu<sub>30</sub>P<sub>20</sub>, Pd<sub>42.5</sub>Ni<sub>7.5</sub>Cu<sub>30</sub>P<sub>20</sub>, Pd<sub>40</sub>Ni<sub>40</sub>P<sub>20</sub>, and Pd<sub>30</sub>Ni<sub>50</sub>P<sub>20</sub> are 580, 571, 586, and 586 K, respectively. Inset: Normalized loss modulus of Pd<sub>40</sub>Ni<sub>10</sub>Cu<sub>30</sub>P<sub>20</sub>, Pd<sub>42.5</sub>Ni<sub>7.5</sub>Cu<sub>30</sub>P<sub>20</sub>, Pd<sub>40</sub>Ni<sub>40</sub>P<sub>20</sub>, and Pd<sub>30</sub>Ni<sub>50</sub>P<sub>20</sub> at 583, 586, 598, and 604 K, respectively. The solid line is a Kohlrausch function with  $\beta_{\text{KWW}} = 0.60$ . For the spectra of Pd<sub>40</sub>Ni<sub>10</sub>Cu<sub>30</sub>P<sub>20</sub> and Pd<sub>40</sub>Ni<sub>40</sub>P<sub>20</sub> to have a superimposition, the spectra were shifted by multiplying the frequency by 1.34 and 1.22, respectively. The  $\beta_{\text{KWW}} = 0.60$  for the four samples are evidently very close.

alloys present very similar phenomena in that of temperature dependence (see Figure 2a). The JG  $\beta$  relaxation is more convoluted with the contribution of the  $\alpha$  relaxation with increasing Ni content. The separation between the  $\alpha$  and  $\beta$  processes as well as their shape as observed in a master curve is not correct, since the two processes have a very different temperature dependence of their shape and relaxation time, so that the TTS over the whole range cannot be valid. However, the master curves are very useful to evidence the differences in the spectra of the investigated glass formers.

In order to characterize the isothermal mechanical spectra, the  $\alpha$  relaxation was described by the Kohlrausch–Williams–Watts (KWW) function<sup>59,60</sup> and the Cole–Cole (CC) equation was used to describe the  $\beta$  process.<sup>61,62</sup>

$$G''(\omega) = \text{Im} \left\{ G_{\infty} + \Delta G_{\alpha} L_{i\omega} \left[ -\frac{d\phi_{\alpha}(t, \tau_{\alpha})}{dt} \right] + \frac{\Delta G_{\beta}}{[1 + (i\omega\tau_{\beta})^b]} \right\} \quad (3)$$

with

$$\phi_{\alpha}(t, \tau_{\alpha}) = \exp[-(t/\tau_{\alpha})^{\beta_{\text{KWW}}}]$$

where  $\beta_{\text{KWW}}$  is the Kohlrausch exponent with values between 0 and 1, reflecting the deviation from the Debye function ( $\beta_{\text{KWW}} = 1$ ).  $\Delta G_{\alpha}$  and  $\Delta G_{\beta}$  are the relaxation strength of the  $\alpha$  relaxation and JG  $\beta$  relaxation, respectively. The parameters  $b$  and  $\beta_{\text{KWW}}$  describe the symmetric and asymmetric broadening of the corresponding spectra. The linear superposition of the two processes as predicted from eq 3 may not be trivial in the case that the relaxation times of two processes are close, and the use of a different ansatz may be necessary. In the spectra analyzed here, the relaxation times of the two processes differ by more than three decades, so this was not an issue.<sup>63,64</sup> Note that, even if in principle eq 3 could be used to analyze the TTS spectra (Figure 5), this was not done in here. As discussed above, the TTS cannot take into account the different temperature dependences of the relaxation times and shapes of the two processes. Thus, the separation and shape of the two processes if determined from the TTS spectra would have a large error especially in the range of temperatures in which the two processes are very close. In here, the TTS spectra are mainly used to show the clearly different relaxation scenarios, not to determine the dynamical properties of the  $\alpha$  and  $\beta$  processes, which were determined only from the isothermal measurements.

We have shown before<sup>62</sup> that eq 3 can be used to fit the master curves (Figure 4), obtaining reasonable values of  $\beta_{\text{KWW}}$ . However, we also pointed out that this cannot be used to determine the relaxation time, since the TTS principle cannot be valid for the whole temperature range. TTS assumes that the shapes of the spectra have to be the same at all temperatures considered; even if we would consider this to be true for the  $\alpha$  and  $\beta$  relaxation separately, this cannot be true for their superposition, since they have very different temperature dependences. However, since the spectra above and below the glass transition temperature  $T_g$  are dominated by the  $\alpha$  and  $\beta$  processes, respectively, we expect that the activation energy obtained from the shift factor (eq 2) is still reasonable, although some deviations are possible if there is a large superposition of two processes.

**3.3. Effect of Aging on the Relaxation Processes in Pd-Based Metallic Glass-Forming Liquids.** Figure 6 presents the shift factor  $a_T$  as a function of isothermal temperature for as-cast and aged samples below the glass transition temperature  $T_g$  (aging temperature 560 K and aging time 4 h, these conditions were chosen empirically to allow the system to relax in a relatively short time). On the basis of eq 2, we determined the apparent activation energy for  $\alpha$  relaxation  $U_{\alpha}$  and Johari–Goldstein relaxation  $U_{\beta}$ .

The values of activation energy for  $U_{\alpha}$  and  $U_{\beta}$  for the as-cast sample are  $5.79 \pm 0.02$  and  $1.31 \pm 0.01$  eV, respectively, and  $6.83 \pm 0.03$  and  $1.30 \pm 0.01$  eV for the aged sample. Let us mention that the as-cast state is an out of equilibrium state and therefore the corresponding values are not really significant,

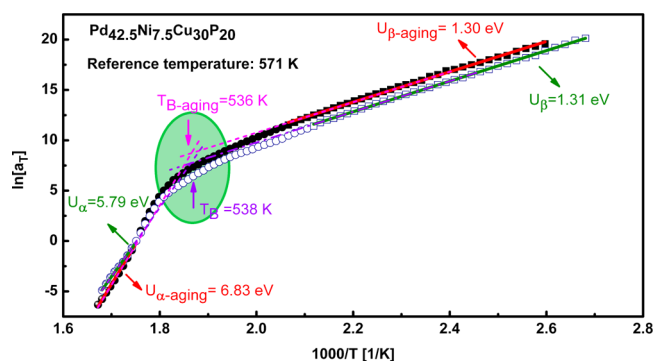


**Figure 6.** Temperature dependence of the shift factor for the as-cast sample and relaxed one in  $\text{Pd}_{42.5}\text{Ni}_{7.5}\text{Cu}_{30}\text{P}_{20}$  bulk metallic glass. The apparent activation energy of  $\alpha$  relaxation and Johari–Goldstein  $\beta$  relaxation are determined by the Arrhenius plots (the solid lines are the Arrhenius plots).

due to a possible evolution of the sample during the experiments. In both cases, the activation energy of  $\alpha$  relaxation of  $\text{Pd}_{42.5}\text{Ni}_{7.5}\text{Cu}_{30}\text{P}_{20}$  metallic glass is about 5 times higher, as expected from the cooperative nature of the atomic motions involved in the  $\alpha$  relaxation. It should be noticed that the value is actually an upper bound, since the activation energy of the  $\beta$  relaxation is often found to increase above  $T_g$ .<sup>65</sup>

The  $\beta$  relaxation in the Pd-based metallic glass-forming liquids corresponds to a diffusion activation energy of P,<sup>66</sup> suggesting that the  $\beta$  process is related to a single atom diffusion. It is interesting to note that the single atom diffusion for P in Cu is 1.41 eV and Pd diffusion in Cu is 2.36 eV, respectively.<sup>67</sup> Therefore, the activation energy JG relaxation in Pd-based metallic glass-forming liquids is very close to the magnitude of the single atom diffusion of P in Cu. Furthermore, the dynamic glass transition in the  $\text{Pd}_{42.5}\text{Ni}_{7.5}\text{Cu}_{30}\text{P}_{20}$  metallic glass is related to around 5 times the cooperative movement of the single atom diffusion of P in Cu.<sup>67</sup> On the basis of current experimental results, the correlation between the apparent activation energy  $U_\beta$  of  $\beta$  relaxation and the glass transition temperature  $T_g$  in  $\text{Pd}_{42.5}\text{Ni}_{7.5}\text{Cu}_{30}\text{P}_{20}$  metallic glass can be established, which is consistent with the empirical law:  $U_\beta \approx 26(\pm 2) RT_g$ . It should be noted that the correlation between the activation energy and

the glass transition temperature  $T_g$  is very similar to that in nonmetallic glassy materials which are  $U_\beta \approx 24 RT_g$ .<sup>68</sup> The activation energy  $U_\beta$  was found to not be sensitive to the physical aging; however, the relaxation time of the  $\beta$  process tends to increase with aging.

In order to study the effect of the physical aging below the glass transition temperature  $T_g$  on the dynamic mechanical relaxation in metallic glass-forming liquids, a comprehensive investigation of isothermal aging was performed at 563 K in  $\text{Pd}_{42.5}\text{Ni}_{7.5}\text{Cu}_{30}\text{P}_{20}$  bulk metallic glass. For isothermal aging, the sample was heated from below  $T_g$  to the aging temperature  $T_a = 563$  K at a constant heating rate of 3 K/min with a driving frequency of 0.3 Hz. Then, the samples were held at this temperature for 4 h. As presented in Figure 7, the physical aging below the glass transition temperature induces an augment of the storage modulus  $G'$  ( $\sim 6\%$ ) and a decrease of the loss factor  $\tan \delta$  and of the loss modulus  $G''$ . The trends reflect the structural relaxation in metallic glass-forming liquids, leading to a decrease of the viscoelastic component and an increase of the elastic component, which is in accordance with the previous publications.<sup>69</sup>

By considering the evolution of the loss factor ( $\tan \delta$ ), we defined the parameter  $\Delta$  function of the aging time,  $t_a$ , as<sup>62,69,70</sup>

$$\Delta = \frac{\tan \delta(t_a) - \tan \delta(t_a \rightarrow \infty)}{\tan \delta(t_a = 0) - \tan \delta(t_a \rightarrow \infty)} \quad (4)$$

The kinetics of the structural relaxation in amorphous materials during aging can be described using the stretched exponential [or Kohlrausch–Williams–Watts (KWW)] relaxation function. The following equation has been introduced to analyze the isothermal aging process in amorphous materials:<sup>62,69,70</sup>

$$\tan \delta(t_a) - \tan \delta(t_a = 0) = A \{1 - \exp[-(t_a/\tau)^{\beta_{\text{aging}}}] \} \quad (5)$$

where  $A$  is the maximum magnitude of the dynamic mechanical relaxation and  $A = \tan \delta(t_a \rightarrow \infty) - \tan \delta(t_a = 0)$ .  $\tau$  is the relaxation time and  $\beta_{\text{aging}}$  is the Kohlrausch exponent with values between 0 and 1, with  $\beta_{\text{aging}} = 1$  corresponding to a single Debye relaxation time. On the basis of eq 5, the relaxation time  $\tau_{\text{aging}}$  and the Kohlrausch exponent  $\beta_{\text{aging}}$  can be obtained (see the solid curve in Figure 7). It should be noted that the Kohlrausch exponent  $\beta_{\text{aging}}$  is about 0.5 for temper-

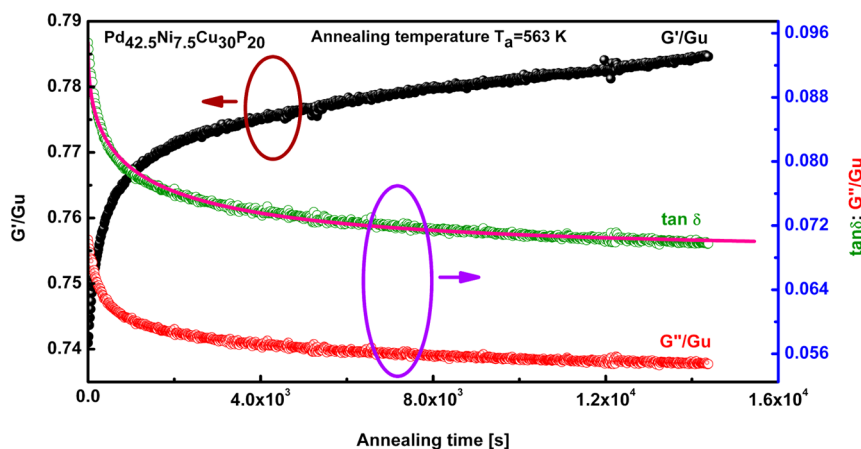


**Figure 7.** Evolution of the storage modulus  $G'$ , loss modulus  $G''$ , and loss factor  $\tan \delta$  for  $\text{Pd}_{42.5}\text{Ni}_{7.5}\text{Cu}_{30}\text{P}_{20}$  bulk metallic glass with the annealing time. The aging temperature is  $T_a = 563$  K, and the driving frequency is 0.3 Hz. The solid curve is best fit from eq 5 obtained for the parameters  $\tau = 1189 \pm 13$  s and  $\beta_{\text{aging}} = 0.447 \pm 0.005$ .

atures close to the glass transition temperature  $T_g$  based on the experimental results<sup>18,62,71–73</sup> as well as the simulation techniques by molecular dynamics (MD).<sup>74</sup> The value of  $\tau$  determined from the fit of the data during aging is reported in Figure 8 together with the relaxation time obtained from the fit

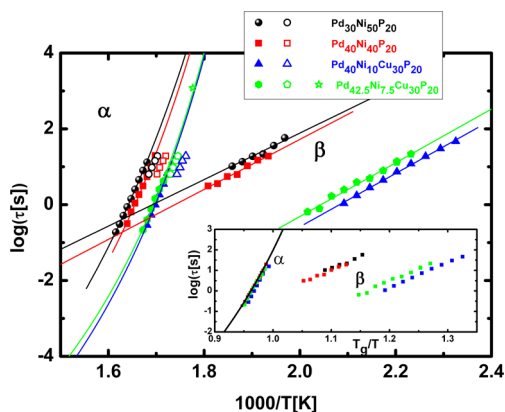


**Figure 8.** Relaxation map for the four investigated metallic glass formers. The solid symbols are from the analysis of the isothermal mechanical spectra using eq 3. The corresponding open symbols were obtained from the modulated DSC measurements (see section 3.4). The solid lines are the best fit to the VFT and Arrhenius equations (parameters in Table 1). The star symbol for  $\text{Pd}_{42.5}\text{Ni}_{7.5}\text{Cu}_{30}\text{P}_{20}$  was obtained from aging measurements. Inset: Fragility plot for the four metallic glass formers. The symbols are the same as the main figure. The four glass formers have steepness index  $59 < m < 67$ .

to the isothermal spectra. The results show that the aging time is very close to the extrapolated value of  $\tau_\alpha$ . This is quite interesting, since even if below the glass transition temperature  $T_g$  the spectra are dominated by the  $\beta$  process their aging is controlled by the  $\alpha$  relaxation.

**3.4. Relaxation Maps in Pd-Based Metallic Glass-Forming Liquids.** The temperature dependence of the  $\alpha$  relaxation time  $\tau_\alpha$  in supercooled liquids is well described by the Vogel–Fulcher–Tamman (VFT) equation:<sup>20</sup>

$$\tau_\alpha = \tau_\infty^\alpha \exp\left(\frac{B}{T - T_0}\right) \quad (6)$$

where the frequency  $\tau_\alpha$  is calculated from the frequency of the peak maximum,  $f_{\text{peak}}$  as  $\tau_\alpha = (2\pi f_{\text{peak}})^{-1}$ ,  $\tau_\infty^\alpha$  is the relaxation time in the limit of high temperatures, and  $T_0$  is the Vogel temperature. A parameter often used in the characterization of amorphous materials is the fragility parameter,  $m = (1/T_g) \left( \frac{\partial \log(\tau)}{\partial (1/T)} \right)_{T_g}$ , which was introduced by Angell.<sup>75–78</sup>

Glass-forming liquids are classified into “strong” and “fragile” if they have small or large  $m$ , respectively. Conceptually, the kinetic fragility parameter  $m$  represents the degree of deviations from the Arrhenius law. Thus, the more “fragile” glass formers

show larger deviations from the Arrhenius equation, while  $\tau_\alpha$  in the stronger glass-forming liquids has a nearly Arrhenius temperature dependence. Normally, metallic glass-forming liquids have intermediate fragility.

From the VFT parameters, the fragility parameter can be calculated as<sup>79,80</sup>

$$m = \frac{BT_g}{\ln 10(T_g - T_0)^2} \quad (7)$$

The relaxation maps in the Pd-based metallic glasses are presented in Figure 8. All four materials show a similar scenario. Above  $T_g$ , the  $\alpha$  process behavior is well described by a VFT equation (solid lines), while, below  $T_g$ , the  $\beta$  process shows an Arrhenius behavior below  $T_g$ .

The  $\alpha$  relaxation for the two systems containing copper ( $\text{Pd}_{42.5}\text{Ni}_{7.5}\text{Cu}_{30}\text{P}_{20}$  and  $\text{Pd}_{40}\text{Ni}_{10}\text{Cu}_{30}\text{P}_{20}$ ) is not affected much from the change of composition. Similarly, there is only a small change in the other two systems ( $\text{Pd}_{40}\text{Ni}_{40}\text{P}_{20}$  and  $\text{Pd}_{30}\text{Ni}_{50}\text{P}_{20}$ ) for a change in the composition of Ni and Pd. The more significant difference is between the two sets of samples, with a decrease of  $T_g$  of about 15 K associated with the substitution of 30% of Ni by Cu. At the same time, we observe that the shape of the  $\alpha$  process is very close for all four materials. In all four cases, a best fit of the loss peak is obtained for  $\beta_{\text{KWW}} = 0.59–0.60$  (Table 1), with a negligible temperature dependence. The independence on composition of the shape of the  $\alpha$  relaxation is also evidenced in the inset of Figure 5.

On the basis of the experimental results in Figure 8, fragility plots for the Pd-based metallic glass-forming liquids are shown in the inset to Figure 8. It can be seen that the fragility for the Cu based systems is higher but the difference is within the experimental error. Calculating the fragility parameter using eq 7, we found  $59 < m < 67$ ; therefore, all the Pd-based metallic glass formers investigated herein are neither strong nor fragile. The relative invariance of  $m$  is in agreement with the correlation between  $\beta_{\text{KWW}}$  and  $m$  observed for Böhmer for many glass formers,<sup>79</sup> although no metallic glasses were included.

In particular, Böhmer et al. found that for most glass formers the dependence of  $m$  on  $\beta_{\text{KWW}}$  is described by<sup>79</sup>

$$m = 250 - 320\beta_{\text{KWW}} \quad (8)$$

In our case, this empirical equation predicts  $58 < m < 61$ , which is very close to the observed values ( $59 < m < 67$ ).

Regarding the secondary relaxation dynamics, it is evident that there is a large difference within the two sets of samples with and without Cu. For the samples in which 30% Ni was substituted with 30% Cu (i.e., from  $\text{Pd}_{40}\text{Ni}_{40}\text{P}_{20}$  to  $\text{Pd}_{40}\text{Ni}_{10}\text{Cu}_{30}\text{P}_{20}$ ), there is a decrease of 2 orders of magnitude of  $\tau_\beta$ . On the other hand, there is almost no change for small substitution (up to 10%) of Ni with Pd.

**Table 1.** Best Fit Parameters of the Vogel–Fulcher–Tamman (VFT) Equation (eq 6) and Arrhenius Equations<sup>a</sup>

metallic glasses	$\log(\tau_\infty^\alpha)$	$B \times 10^2$ (K)	$T_0$ (K)	$T_g^\alpha$ (K)	$m$	$\beta_{\text{KWW}}$	$\log(\tau_\beta^\infty)$	$U_\beta$ (eV)	$U_\beta/RT_g$
$\text{Pd}_{40}\text{Ni}_{10}\text{Cu}_{30}\text{P}_{20}$	$-13.3 \pm 1.3$	$45 \pm 5$	$440 \pm 9$	$570 \pm 3$	$66 \pm 7$	$0.60 \pm 0.01$	$-14.6 \pm 0.2$	$1.39 \pm 0.02$	$28 \pm 0.2$
$\text{Pd}_{30}\text{Ni}_{50}\text{P}_{20}$	$-14.6 \pm 1$	$65 \pm 6$	$416 \pm 11$	$586 \pm 4$	$57 \pm 6$	$0.59 \pm 0.01$	$-10.4 \pm 0.6$	$1.22 \pm 0.07$	$25 \pm 0.2$
$\text{Pd}_{40}\text{Ni}_{40}\text{P}_{20}$	$-13.5 \pm 1$	$53 \pm 5$	$433 \pm 10$	$582 \pm 4$	$60 \pm 6$	$0.59 \pm 0.01$	$-11.5 \pm 0.7$	$1.31 \pm 0.07$	$26 \pm 0.2$
$\text{Pd}_{42.5}\text{Ni}_{7.5}\text{Cu}_{30}\text{P}_{20}$	$-12.2 \pm 1.1$	$39 \pm 4$	$450 \pm 9$	$569 \pm 3$	$69 \pm 7$	$0.60 \pm 0.01$	$-14.5 \pm 0.5$	$1.40 \pm 0.04$	$28 \pm 0.2$

<sup>a</sup>The fragility index was calculated by using eq 7. The glass temperature  $T_g^\alpha$  is the temperature at which  $\tau_\alpha = 100$  s.

Therefore, both the master curves and the fit to the isothermal spectra are consistent with an increase of about two decades in the separation between the  $\alpha$  and  $\beta$  processes for the metallic glass-forming liquids with Cu. However, only small changes in the temperature dependence and shape of the  $\alpha$  process are observed between the studied metallic glasses. Thus, there is not an evident connection between the  $\alpha$  and  $\beta$  relaxations.

**3.5. MDSC Measurements of Pd-Based Metallic Glass-Forming Liquids.** The real and imaginary parts of the heat capacity,  $c_p'$  and  $c_p''$ , are shown for the four metallic glass formers in Figure 9 (temperature modulation period  $T_m = 90$  s).  $c_p'$  and

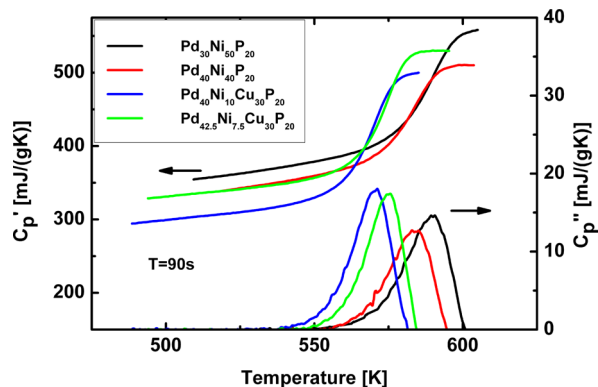


**Figure 9.** Real and imaginary parts of the heat capacity of the four Pd-based metallic glass formers for a 90 s temperature modulation period.

$c_p''$  were calculated from the reversible heat capacity and heat flow phase after correction of the heat flow phase, as discussed by Weyer et al.<sup>81</sup> The breadth,  $2\delta T$ , and the temperature of maximum,  $T^*$ , of  $c_p''$  were determined by fitting a Gaussian function to the peaks of  $c_p''$  and  $\partial c_p''/\partial T$ . Defining the relaxation time  $\tau^* = (2\pi/T_m)^{-1}$ , with  $T_m$  the period of the temperature modulation, at the temperature  $T^*$  of the peak of  $c_p''$ , we calculated the  $\tau^*(T^*)$  reported in Figure 8. The relaxation times,  $\tau^*$ , from the MDSC are all smaller than the mechanical relaxation time extracted from the analysis of the isothermal spectra. It should be noted that, because of the temperature dependence of the loss peak amplitude, when comparing  $\tau$  from isothermal spectra with the  $\tau$  obtained from isochronal measurements (i.e., Figure 2), the latter is smaller,<sup>64</sup> and the relaxation time  $\tau^*$  is analogous to the  $\tau$  obtained from isochronal measurements. As shown in Figure 10, in our case, we see that by a small shift in temperature  $3.5 \text{ K} < T_{\text{shift}} < 7 \text{ K}$  (Table 2), constant for each set of data, it is possible to superimpose the MDSC relaxation data with the mechanical relaxation data.<sup>82</sup>

The breadth of the peak in isochronal measurements is determined by the breadth of the peak in isothermal spectra (related to  $\beta_{\text{KWW}}$ ) and the temperature dependence of the relaxation time by<sup>83</sup>

$$\begin{aligned} \delta T &\approx \frac{-1.07T}{\beta_{\text{KWW}}} \left( \frac{\partial \ln \tau_\alpha}{\partial \ln T} \right)^{-1} \\ &= \frac{1.07T^2}{\beta_{\text{KWW}}} \left( \frac{\partial \ln \tau_\alpha}{\partial 1/T} \right)^{-1} \\ &= \frac{1.07T}{\beta_{\text{KWW}} \ln(10)m} \end{aligned} \quad (9)$$

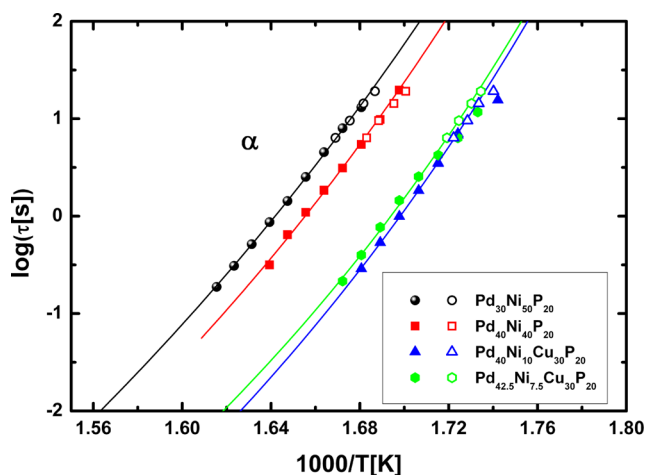


**Figure 10.** Relaxation map for the four investigated metallic glass formers. The solid symbols are from the analysis of the isothermal mechanical spectra using eq 3 (same as Figure 8). The corresponding open symbols were obtained from the modulated DSC measurements; in this case, the temperature of each set of data was shifted by a different  $T_{\text{shift}}$  (Table 2) to superimpose the MDSC data with the mechanical data. The solid lines are the best fit to the VFT and Arrhenius equations (parameters in Table 1).

Using this equation, we calculated the  $\beta_{\text{KWW}}^{\text{MDSC}}$  for the MDSC measurements from the measured  $\delta T$  and the fragility index from the mechanical measurements. The values of  $\beta_{\text{KWW}}^{\text{MDSC}}$  (Table 2) are very close to those from the fit to be isothermal mechanical spectra  $\beta_{\text{KWW}}$  (Table 1), again confirming that the  $\beta_{\text{KWW}}$  for the studied metallic glasses is not very dependent on their composition.

**3.6. Dynamic Heterogeneity.** The dynamics of supercooled liquids is thought to be spatially heterogeneous. With decreasing temperature (or increasing density), the length scale of the dynamic correlation length increases, causing the slowing down of the dynamics that eventually bring the glass transition. Since within the regions of correlated motion regions of slow and fast dynamics coexist, ultimately with decreasing temperature also the heterogeneity increases. On approaching the glass transition, the size of the regions of cooperativity (i.e., the length of cooperativity) grows, and within these, regions of slow and fast dynamics coexist. To determine experimentally the number of units within a correlating region, different metrics have been proposed.

Donth has proposed that the number of correlating units (i.e., atoms in a metallic glass, segments in a polymer, molecules in a simple liquid) can be determined from thermodynamic quantities as<sup>84</sup>

$$N_\alpha = \frac{RT^2}{m_0(\delta T)^2} \Delta c_p^{-1} \quad (10)$$

where  $m_0$  is the molecular weight of the relaxing unit and  $\delta T$  can be determined from  $c_p''$  as discussed above. In this case, since we are considering an alloy, it is not correct to define a molecular weight but instead we calculated the average molecular weight based on the alloy composition. The values of  $N_\alpha$  calculated using eq 10 with the measured thermodynamic properties at the longest measured  $\tau^*$  ( $=19.1$  s) are reported in Table 2. We found  $N_\alpha \sim 600$  for the metallic glass-forming liquids without Cu and  $N_\alpha \sim 1100$  for the metallic glass with Cu. Interestingly, these values are significantly larger than those

Table 2. Thermodynamic Quantities Measured Using MDSC

metallic glass formers	$T^*$ (K)	$\delta T$ (K)	$c_p^{\text{glass}}$ [J/(gK)]	$c_p^{\text{liquid}}$ [J/(gK)]	$\Delta c_p^{-1}$ [(gK)/J]	$N_\alpha$	$N_c^{\text{MDSC}}$	$N_c^{\text{G}^r}$	$\beta_{\text{KWW}}^{\text{MDSC}}$	$T_{\text{shift}}$ (K)
Pd <sub>40</sub> Ni <sub>10</sub> Cu <sub>30</sub> P <sub>20</sub>	294.5 ± 0.3	6.5 ± 0.1	0.33 ± 0.01	0.55 ± 0.01	1.2 ± 0.06	1040 ± 80	730 ± 70	710 ± 70	0.61 ± 0.01	7
Pd <sub>30</sub> Ni <sub>30</sub> P <sub>20</sub>	314.2 ± 0.3	7.6 ± 0.1	0.40 ± 0.01	0.54 ± 0.01	0.65 ± 0.03	570 ± 40	960 ± 90	940 ± 90	0.62 ± 0.01	5.5
Pd <sub>40</sub> Ni <sub>40</sub> P <sub>20</sub>	312.6 ± 0.3	7.5 ± 0.1	0.39 ± 0.01	0.51 ± 0.01	0.60 ± 0.03	590 ± 50	1100 ± 100	1060 ± 100	0.61 ± 0.01	6.5
Pd <sub>42.5</sub> Ni <sub>7.5</sub> Cu <sub>30</sub> P <sub>20</sub>	299.6 ± 0.3	6.5 ± 0.1	0.38 ± 0.01	0.55 ± 0.01	0.82 ± 0.04	1090 ± 80	970 ± 90	1000 ± 100	0.59 ± 0.01	3.5

found for polymers and molecular liquids for which generally  $N_\alpha < 400$ .<sup>85</sup>

Using a different approach, Berthier et al.<sup>86,87</sup> have derived an approximate formula for the number of correlated units

$$N_c = \frac{R}{\Delta c_p} T^2 \left\{ \max_t \chi_T(t) \right\}^2 \quad (11)$$

where  $\chi_T$  is the time derivative of a suitable correlation function. In this case, the correlation function has a stretched exponential form (like in eq 3 for the  $\alpha$  relaxation) and it has been shown that it reduces to<sup>88</sup>

$$N_c = \frac{R}{\Delta c_p m_0} \left( \frac{\beta_{\text{KWW}}}{e} \right)^2 \left( \frac{\partial \ln \tau_\alpha}{\partial \ln T} \right)^2 \quad (12)$$

where  $e$  is the Euler number. The values of  $N_c$  calculated using eq 11 from the mechanical measurements are reported in Table 2.  $N_c$  can be calculated from the thermodynamic data.

Taking into consideration eqs 9, 10, and 12, it follows that<sup>64</sup>

$$\frac{N_\alpha}{N_c} \approx 6.45 \Delta c_p \Delta c_p^{-1} \quad (13)$$

For the cases included herein,  $0.07 < \Delta c_p \Delta c_p^{-1} < 0.14$ ; thus,  $0.45 < N_\alpha/N_c < 0.9$ . The values of  $N_c$  calculated from the thermodynamic quantities using eq 13 are reported in Table 2 ( $N_c^{\text{MDSC}}$ ), and we can see that the values are very close to those found from the dynamics (i.e., eq 12).

Like for the values of  $N_\alpha$ , also the values of  $N_c$  are significantly larger than those observed for other types of glass formers, for which  $N_c < 570$ .<sup>88</sup> These large values of  $N_\alpha$  and  $N_c$  for metallic glass-forming liquids could indicate the existence of a short-range order in metallic glasses; that is, atoms in metallic glasses could be organized into clusters, instead of moving independently.<sup>89</sup> To our knowledge, the determination of  $N_\alpha$  and  $N_c$  has not been carried out for other metallic glass-forming liquids, so it is not yet clear how general this result is.

#### 4. CONCLUSIONS

The dynamics of four Pd-based metallic glass formers was investigated by mechanical spectroscopy (DMA) and modulated differential scanning calorimetry (MDSC). For the materials considered herein, we found that the change in composition has a significant effect on the  $\alpha$  relaxation dynamics. With the largest difference showing an increase of  $T_g$  for materials in which 30%Ni was substituted by 30%Cu. All four materials have very similar fragility parameters,  $59 < m < 67$ , and similar stretched exponents,  $0.59 < \beta_{\text{KWW}} < 0.6$ . Interestingly, the values of  $\beta_{\text{KWW}}$  and  $m$  are in good agreement with that found by Böhmer et al. for nonmetallic glass formers.<sup>79</sup> The correlation found by Böhmer et al. for the observed value of  $\beta_{\text{KWW}}$  predicts  $58 < m < 61$ . The substitution of Ni with Cu has a very large effect on the  $\beta$  relaxation of the metallic glasses, with the  $\tau_\beta$  relaxation more than 2 orders of magnitude smaller in the metallic glass with Cu. Notwithstand-

ing the difference in the activation energy,  $U_\beta$  of the  $\beta$  relaxation is quite close and in all cases it was found  $25 < U_\beta/RT < 28$ , which agrees with previous results for other glass formers.<sup>68,90</sup>

The number of correlated relaxing units was estimated from both mechanical and MDSC measurements, finding consistent results. The number of correlated units is found to be significantly larger than that for other glass formers; this could be indicative of a short-range order in metallic glass-forming liquids.

#### AUTHOR INFORMATION

##### Corresponding Author

\*Phone: +33 4 72 43 83 18. Fax: +33 4 72 43 85 28. E-mail: jean-marc.pelletier@insa-lyon.fr.

##### Notes

The authors declare no competing financial interest.

#### ACKNOWLEDGMENTS

One of the authors, J.Q., would like to thank the Centre National de la Recherche Scientifique (CNRS) for providing the postdoctoral financial support. In addition, J.Q. appreciates Dr. N. Nishiyama and Dr. T. Wada for preparing the Pd-based metallic glass formers at Tohoku University, Japan. R.C. acknowledges the support of the Office of Naval Research for the work at NRL.

#### REFERENCES

- (1) Wang, W. H. The Elastic Properties, Elastic Models and Elastic Perspectives of Metallic Glasses. *Prog. Mater. Sci.* **2012**, *57*, 487–656.
- (2) Roland, C. M. *Viscoelastic Behavior of Rubbery Materials*; Oxford: New York, 2011.
- (3) Pelletier, J. M.; Louzguine-Luzgin, D. V.; Li, S.; Inoue, A. Elastic and Viscoelastic Properties of Glassy, Quasicrystalline and Crystalline Phases in Zr<sub>65</sub>Cu<sub>5</sub>Ni<sub>10</sub>Al<sub>7.5</sub>Pd<sub>12.5</sub> Alloys. *Acta Mater.* **2011**, *59*, 2797–2806.
- (4) Zuriaga, M.; Pardo, L. C.; Lunkenheimer, P.; Tamarit, J. L.; Veglio, N.; Barrio, M.; Bermejo, F. J.; Loidl, A. New Microscopic Mechanism for Secondary Relaxation in Glasses. *Phys. Rev. Lett.* **2009**, *103*, 075701.
- (5) Ngai, K. L.; Wang, Z.; Gao, X. Q.; Yu, H. B.; Wang, W. H. A Connection between the Structural  $\alpha$ -relaxation and the  $\beta$ -relaxation Found in Bulk Metallic Glass-Formers. *J. Chem. Phys.* **2013**, *139*, 014502.
- (6) Yu, H. B.; Samwer, K.; Wang, W. H.; Bai, H. Y. Chemical Influence on  $\beta$ -relaxations and the Formation of Molecule-like Metallic Glasses. *Nat. Commun.* **2013**, *4*, 2204.
- (7) Qiao, J. C.; Pelletier, J. M. Dynamic Mechanical Analysis in La-based Bulk Metallic Glasses: Secondary ( $\beta$ ) and Main ( $\alpha$ ) Relaxations. *J. Appl. Phys.* **2012**, *112*, 083528.
- (8) Qiao, J. C.; Pelletier, J. M. Enthalpy Relaxation in Cu<sub>46</sub>Zr<sub>45</sub>Al<sub>7</sub>Y<sub>2</sub> and Zr<sub>55</sub>Cu<sub>30</sub>Ni<sub>5</sub>Al<sub>10</sub> Bulk Metallic Glasses by Differential Scanning Calorimetry (DSC). *Intermetallics* **2011**, *19*, 9–18.
- (9) Haruyama, O.; Nakayama, Y.; Wada, R.; Tokunaga, H.; Okada, J.; Ishikawa, T.; Yokoyama, Y. Volume and Enthalpy Relaxation in Zr<sub>55</sub>Cu<sub>30</sub>Ni<sub>5</sub>Al<sub>10</sub> Bulk Metallic Glass. *Acta Mater.* **2010**, *58*, 1829–1836.

- (10) Fan, G. J.; Löffler, J. F.; Wunderlich, R. K.; Fecht, H. J. Thermodynamics, Enthalpy Relaxation and Fragility of the Bulk Metallic Glass-Forming Liquid Pd<sub>43</sub>Ni<sub>10</sub>Cu<sub>27</sub>P<sub>20</sub>. *Acta Mater.* **2004**, *52*, 667–674.
- (11) Haruyama, O.; Sawada, H.; Yoshikawa, K.; Kawamata, T.; Yokoyama, Y.; Sugiyama, K. Static Measurements for  $\alpha$ - and  $\beta$ -relaxation below  $T_g$  in a Zr<sub>55</sub>Cu<sub>30</sub>Ni<sub>5</sub>Al<sub>10</sub> BMG. *TMS 2013, Annu. Meet. Exhib., Suppl. Proc., 142nd* **2013**, 273–280.
- (12) Xue, R. J.; Wang, D. P.; Zhu, Z. G.; Ding, D. W.; Zhang, B.; Wang, W. H. Characterization of Flow Units in Metallic Glass Through Density Variation. *J. Appl. Phys.* **2013**, *114*, 123514.
- (13) Evenson, Z.; Schmitt, T.; Nicola, M.; Gallino, I.; Busch, R. High Temperature Melt Viscosity and Fragile to Strong Transition in Zr–Cu–Ni–Al–Nb(Ti) and Cu<sub>47</sub>Ti<sub>34</sub>Zr<sub>11</sub>Ni<sub>8</sub> Bulk Metallic Glasses. *Acta Mater.* **2012**, *60*, 4712–4719.
- (14) Evenson, Z.; Busch, R. Equilibrium Viscosity, Enthalpy Recovery and Free Volume Relaxation in a Zr<sub>44</sub>Ti<sub>11</sub>Ni<sub>10</sub>Cu<sub>10</sub>Be<sub>25</sub> Bulk Metallic Glass. *Acta Mater.* **2011**, *59*, 4404–4415.
- (15) Pineda, E.; Bruna, P.; Ruta, B.; Gonzalez-Silveira, M.; Crespo, D. Relaxation of Rapidly Quenched Metallic Glasses: Effect of the Relaxation State on the Slow Low Temperature Dynamics. *Acta Mater.* **2013**, *61*, 3002–3011.
- (16) Hachenberg, J.; Bedorf, D.; Samwer, K.; Richert, R.; Kahl, A.; Demetriou, M. D.; Johnson, W. L. Merging of the  $\alpha$  and  $\beta$  Relaxations and Aging via Johari–Goldstein Modes in Rapidly Quenched Metallic Glasses. *Appl. Phys. Lett.* **2008**, *92*, 131911.
- (17) Wang, Z.; Wen, P.; Huo, L. S.; Bai, H. Y.; Wang, W. H. Signature of Viscous Flow Units in Apparent Elastic Regime of Metallic Glasses. *Appl. Phys. Lett.* **2012**, *101*, 121906.
- (18) Wang, L. M.; Liu, R. P.; Wang, W. H. Relaxation Time Dispersions in Glass Forming Metallic Liquids and Glasses. *J. Chem. Phys.* **2008**, *128*, 164503.
- (19) Kristiakova, K.; Svec, P.; Kristiak, J.; Duhaj, P.; Sausa, O. Short Range Ordering in the Melt and Its Manifestation in Glassy Fe–Co–B - Investigation by Positron Annihilation Lifetime. *Mater. Sci. Eng., A* **1997**, *226*, 321–325.
- (20) Johari, G. P.; Khouri, J. Non-exponential Nature of Calorimetric and Other Relaxations: Effects of 2 nm-size Solutes, Loss of Translational Diffusion, Isomer Specificity, and Sample Size. *J. Chem. Phys.* **2008**, *138*, 12A511.
- (21) Johari, G. P.; Goldstein, M. Viscous Liquids and the Glass Transition. II. Secondary Relaxations in Glasses of Rigid Molecules. *J. Chem. Phys.* **1970**, *53*, 2372–2388.
- (22) Yu, H. B.; Wang, W. H.; Samwer, K. The  $\beta$  Relaxations in Metallic Glasses: An Overview. *Mater. Today* **2013**, *16*, 183–191.
- (23) Yu, H. B.; Wang, W. H.; Bai, H. Y.; Wu, Y.; Chen, M. W. Relating Activation of Shear Transformation Zones to  $\beta$  Relaxations in Metallic Glasses. *Phys. Rev. B* **2010**, *81*, 220201.
- (24) Zhang, C. Z.; Hu, L. N.; Yue, Y. Z.; Mauro, J. C. Fragile-to-strong Transition in Metallic Glass-forming Liquids. *J. Chem. Phys.* **2010**, *133*, 014508.
- (25) Hu, L. N.; Yue, Y. Z. Secondary Relaxation in Metallic Glass Formers: Its Correlation with the Genuine Johari–Goldstein Relaxation. *J. Phys. Chem. C* **2009**, *113*, 15001–15006.
- (26) Hu, L. N.; Yue, Y. Z. Secondary Relaxation Behavior in a Strong Glass. *J. Phys. Chem. B* **2008**, *112*, 9053–9057.
- (27) Yang, H. W.; Tong, W. P.; Zhao, X.; Zuo, L.; Wang, J. Q. Observation of  $\beta$ -Relaxation in Sub- $T_g$  Isothermally Annealed Al-Based Metallic Glasses. *Chin. Phys. Lett.* **2008**, *25*, 3357–3359.
- (28) Okumura, H.; Inoue, A.; Masumoto, T. Glass Transition and Viscoelastic Behaviors of La<sub>55</sub>Al<sub>25</sub>Ni<sub>20</sub> and La<sub>55</sub>Al<sub>25</sub>Cu<sub>20</sub> Amorphous Alloys. *Mater. Trans., JIM* **1991**, *32*, 593–598.
- (29) Okumura, H.; Inoue, A.; Masumoto, T. Heating Rate Dependence of Two Glass Transitions and Phase Separation for a La<sub>55</sub>Al<sub>25</sub>Ni<sub>20</sub> Amorphous Alloy. *Acta Metall. Mater.* **1993**, *41*, 915–921.
- (30) Okumura, H.; Chen, H. S.; Inoue, A.; Masumoto, T. Sub- $T_g$  Mechanical Relaxation of a La<sub>55</sub>Al<sub>25</sub>Ni<sub>20</sub> Amorphous Alloy. *J. Non-Cryst. Solids* **1991**, *130*, 304–310.
- (31) Wang, Z.; Yu, H. B.; Wen, P.; Bai, H. Y.; Wang, W. H. Pronounced Slow  $\beta$ -Relaxation in La-based Bulk Metallic Glasses. *J. Phys.: Condens. Matter* **2011**, *23*, 142202.
- (32) Qiao, J. C.; Pelletier, J. M.; Kou, H. C.; Zhou, X. Modification of Atomic Mobility in a Ti-based Bulk Metallic Glass by Plastic Deformation or Thermal Annealing. *Intermetallics* **2012**, *28*, 128–137.
- (33) Struik, L. C. E. Physical Aging in Plastics and Other Glassy Materials. *Polym. Eng. Sci.* **1977**, *17*, 165–173.
- (34) Casalini, R.; Roland, C. M. Aging of the Secondary Relaxation to Probe Structural Relaxation in the Glassy State. *Phys. Rev. Lett.* **2009**, *102*, 035701.
- (35) Lunkenheimer, P.; When, R.; Schneider, U.; Loidl, A. Glassy Aging Dynamics. *Phys. Rev. Lett.* **2005**, *95*, 055702.
- (36) Pelletier, J. M.; Van de Moortèle, B.; Lu, I. R. Viscoelasticity and Viscosity of Pd–Ni–Cu–P Bulk Metallic Glasses. *Mater. Sci. Eng., A* **2002**, *336*, 190–195.
- (37) Ichitsubo, T.; Matsubara, E.; Yamamoto, T.; Chen, H. S.; Nishiyama, N.; Saida, J.; Anazawa, K. Microstructure of Fragile Metallic Glasses Inferred from Ultrasound-Accelerated Crystallization in Pd-Based Metallic Glasses. *Phys. Rev. Lett.* **2005**, *95*, 245501.
- (38) Ichitsubo, T.; Matsubara, E.; Chen, H. S.; Saida, J.; Yamamoto, T.; Nishiyama, N. Structural Instability of Metallic Glasses Under Radio-frequency-Ultrasonic Perturbation and its Correlation with Glass-to-Crystal Transition of Less-Stable Metallic glasses. *J. Chem. Phys.* **2006**, *125*, 154502.
- (39) Liu, Y. H.; Wang, G.; Wang, R. J.; Zhao, D. Q.; Pan, M. X.; Wang, W. H. Super Plastic Bulk Metallic Glasses at Room Temperature. *Science* **2007**, *315*, 1385–1388.
- (40) Yu, H. B.; Shen, X.; Wang, Z.; Gu, L.; Wang, W. H.; Bai, H. Y. Tensile Plasticity in Metallic Glasses with Pronounced  $\beta$  Relaxations. *Phys. Rev. Lett.* **2012**, *108*, 015504.
- (41) Eckert, J.; Das, J.; Pauly, J.; Duhamel, C.; Kim, K. B.; Yi, S.; Wang, W. H. Impact of Microstructural Inhomogeneities on the Ductility of Bulk Metallic Glasses. *Mater. Trans.* **2007**, *48*, 1806–1811.
- (42) Liu, Y. H.; Wang, D.; Nakajima, K.; Zhang, W.; Hirata, A.; Nishi, T.; Inoue, A.; Chen, M. W. Experimental Characterization of Nanoscale Mechanical Heterogeneity in a Metallic Glass. *Phys. Rev. Lett.* **2011**, *106*, 125504.
- (43) Fujita, T.; Guan, P. F.; Sheng, H. W.; Sakurai, T.; Chen, M. W. Coupling between Chemical and Dynamic Heterogeneities in a Multicomponent Bulk Metallic Glass. *Phys. Rev. B* **2010**, *81*, 140204 (R).
- (44) Tanaka, H.; Kawasaki, T.; Shintani, H.; Watanabe, K. Critical-like Behaviour of Glass-Forming Liquids. *Nat. Mater.* **2010**, *9*, 324–331.
- (45) Casalini, R.; Snow, A. W.; Roland, C. M. Temperature Dependence of the Johari–Goldstein Relaxation in Poly(methyl methacrylate) and Poly(thiomethyl methacrylate). *Macromolecules* **2013**, *46*, 330–334.
- (46) Nishiyama, N.; Inoue, A. Glass-forming Ability of Bulk Pd<sub>40</sub>Ni<sub>10</sub>Cu<sub>30</sub>P<sub>20</sub> Alloy. *Mater. Trans., JIM* **1996**, *37*, 1531–1539.
- (47) Etienne, S.; Cavaillé, J. Y.; Perez, J.; Point, R.; Salvia, M. Automatic System for Analysis of Micromechanical Properties. *Rev. Sci. Instrum.* **1982**, *53*, 1261–1266.
- (48) Cole, K. S.; Cole, R. H. Dispersion and Absorption in Dielectrics - I Alternating Current Characteristics. *J. Chem. Phys.* **1941**, *9*, 341–352.
- (49) Turnbull, D.; Cohen, M. H. Free-Volume Model of the Amorphous Phase: Glass Transition. *J. Chem. Phys.* **1961**, *34*, 120–125.
- (50) Turnbull, D.; Cohen, M.H.. On the Free-Volume Model of the Liquid-Glass Transition. *J. Chem. Phys.* **1970**, *52*, 3038–3041.
- (51) Egami, T.; Levashov, V.; Aga, R. S.; Morris, J. R. Atomic Dynamics in Metallic Liquids and Glasses. *Mater. Trans.* **2007**, *48*, 1729–1733; *Mater. Sci. Eng., A* **2009**, *527*, 1–6.
- (52) Egami, T.; Poon, S. J.; Zhang, Z.; Keppens, V. Glass Transition in Metallic Glasses: A Microscopic Model of Topological Fluctuations in the Bonding Network. *Phys. Rev. B* **2007**, *76*, 024203.

- (53) Perez, J.; Cavaillé, J. Y.; Etienne, S.; Fouquet, F.; Guyot, F. Internal Friction in Vitreous Solid to Glass Transition. *Ann. Phys.* **1983**, *8*, 417–467.
- (54) Perez, J. Quasi-Punctual Defects in Vitreous Solids and Liquid-Glass Transition. *Solid State Ionics* **1990**, *39*, 69–79.
- (55) Perez, J. Defect Diffusion Model for Volume and Enthalpy Recovery in Amorphous Polymers. *Polymer* **1988**, *29*, 483–489.
- (56) Perez, J. *Matériaux Non Cristallins et Science du Désordre*; Presses polytechniques et universitaires romandes: Lausanne, Switzerland, 2001.
- (57) Jeong, H. T.; Park, J. M.; Kim, W. T.; Kim, D. H. Quasicrystalline Effects on the Mechanical Relaxation Behavior of a  $\text{Ti}_{42}\text{Zr}_{16}\text{Ni}_9\text{Cu}_{10}\text{Be}_{20}$  Metallic Glass. *Mater. Sci. Eng., A* **2009**, *527*, 1–6.
- (58) Schröter, K.; Wilde, G.; Willnecker, R.; Weiss, M.; Samwer, K.; Donth, E. Shear Modulus and Compliance in the Range of the Dynamic Glass Transition for Metallic Glasses. *Eur. Phys. J. B* **1998**, *5*, 1–5.
- (59) Zhao, Z. F.; Wen, P.; Shek, C. H.; Wang, W. H. Measurements of Slow  $\beta$ -relaxation in Metallic Glasses and Supercooled Liquids. *Phys. Rev. B* **2007**, *75*, 174201.
- (60) Wen, P.; Zhao, D. Q.; Pan, M. X.; Wang, W. H.; Huang, Y. P.; Guo, M. L. Relaxation of Metallic  $\text{Zr}_{46.75}\text{Ti}_{8.25}\text{Cu}_{7.5}\text{Ni}_{10}\text{Be}_{27.5}$  Bulk Glass-forming Supercooled Liquid. *Appl. Phys. Lett.* **2004**, *84*, 2790–2792.
- (61) McCrum, N. G.; Read, B. E.; Williams, G. *Anelastic and Dielectric Effects in Polymeric Solids*; Wiley: New York, 1967.
- (62) Qiao, J. C.; Pelletier, J. M.; Casalini, R. Relaxation of Bulk Metallic Glasses studied by Mechanical Spectroscopy. *J. Phys. Chem. B* **2013**, *117*, 13658–13666.
- (63) Casalini, R.; Roland, C. M. Density Scaling of the Structural and Johari–Goldstein Secondary Relaxations in Poly(methyl methacrylate). *Macromolecules* **2013**, *46*, 6364–6368.
- (64) Casalini, R.; Fragiadakis, D.; Roland, C. M. Relaxation Dynamics of Poly(methyl acrylate) at Elevated Pressure. *Macromolecules* **2011**, *44*, 6928–6934.
- (65) Paluch, M.; Roland, C. M.; Pawlus, S.; Ziolo, J.; Ngai, K. L. Does the Arrhenius Temperature Dependence of the Johari–Goldstein Relaxation Persist above  $T_g$ ? *Phys. Rev. Lett.* **2003**, *91*, 115701.
- (66) Yu, H. B.; Samwer, K.; Wu, Y.; Wang, W. H. Correlation between  $\beta$  Relaxation and Self-Diffusion of the Smallest Constituting Atoms in Metallic Glasses. *Phys. Rev. Lett.* **2012**, *109*, 095508.
- (67) (a) Japan Institute of Metals. *Metal Data Book*, 4th ed.; Maruzen: Sendai, Japan, 2004. (b) Kato, T.; Ichitsubo, T.; Wang, H.; Wada, T. Dynamic Relaxation of  $\text{Pd}_{42.5}\text{Ni}_{7.5}\text{Cu}_{30}\text{P}_{20}$  Metallic Glass. *J. Jpn. Soc. Powder Metall.* **2013**, *60*, 228–235.
- (68) Kudlik, A.; Tschirwitz, C.; Benkhof, S.; Blochowicz, T.; Rossler, E. Slow Secondary Relaxation Process in Supercooled Liquids. *Europhys. Lett.* **1997**, *40*, 649–654.
- (69) Qiao, J. C.; Pelletier, J. M. Kinetics of Structural Relaxation in Bulk Metallic Glasses by Mechanical Spectroscopy: Determination of the Stretching Parameter  $\beta_{\text{KWW}}$ . *Intermetallics* **2012**, *28*, 40–44.
- (70) Pelletier, J. M. Influence of Structural Relaxation on Atomic Mobility in a  $\text{Zr}_{41.2}\text{Ti}_{13.8}\text{Cu}_{12.5}\text{Ni}_{10.0}\text{Be}_{22.5}$  (Vit1) Bulk Metallic Glass. *J. Non-Cryst. Solids* **2008**, *354*, 3666–3670.
- (71) (a) Qiao, J. C.; Pelletier, J. M. Mechanical Relaxation in a Zr-based Bulk Metallic Glass: Analysis Based on Physical Models. *J. Appl. Phys.* **2012**, *112*, 033518. (b) Qiao, J. C.; Pelletier, J. M. Dynamic Universal Characteristic of the Main ( $\alpha$ ) Relaxation in Bulk Metallic Glasses. *J. Alloys Compd.* **2014**, *589*, 263–270.
- (72) Ngai, K. L.; Yu, H. B. Origin of Ultrafast Ag Radiotracer Diffusion in Shear Bands of Deformed Bulk Metallic Glass  $\text{Pd}_{40}\text{Ni}_{40}\text{P}_{20}$ . *J. Appl. Phys.* **2013**, *113*, 103508.
- (73) Wang, L. M.; Chen, Z. M.; Zhao, Y.; Liu, R. P.; Tian, Y. J. Non-exponentiality of Structural Relaxations in Glass Forming Metallic Liquids. *J. Alloys Compd.* **2010**, *504*, S201–S204.
- (74) Mayr, S. G. Relaxation Kinetics and Mechanical Stability of Metallic Glasses and Supercooled Melts. *Phys. Rev. B* **2009**, *79*, 060201.
- (75) Angell, C. A. Formation of Glasses from Liquids and Biopolymers. *Science* **1995**, *267*, 1924–1935.
- (76) Angell, C. A. Relaxation in Liquids, Polymers and Plastic Crystals: Strong/Fragile Patterns and Problems. *J. Non-Cryst. Solids* **1991**, *131–133*, 13–31.
- (77) Angell, C. A. Perspective on the Glass Transition. *J. Phys. Chem. Solids* **1988**, *49*, 863–871.
- (78) Angell, C. A. Spectroscopy Simulation and Scattering, and the Medium Range Order Problem in Glass. *J. Non-Cryst. Solids* **1985**, *73*, 1–17.
- (79) Böhmer, R.; Ngai, K. L.; Angell, C. A.; Plazek, D. J. Nonexponential Relaxations in Strong and Fragile Glass Formers. *J. Chem. Phys.* **1993**, *99*, 4201–4209.
- (80) Jeong, H. T.; Fleury, E.; Kim, W. T.; Kim, D. H.; Hono, K. Study on the Mechanical Relaxations of a  $\text{Zr}_{36}\text{Ti}_{24}\text{Be}_{40}$  Amorphous Alloy by Time–Temperature Superposition Principle. *J. Phys. Soc. Jpn.* **2004**, *73*, 3192–3197.
- (81) Weyer, S.; Hensel, A.; Schick, C. Phase Angle Correction for TMDSC in the Glass-Transition Region. *Thermochim. Acta* **1997**, *304–305*, 267–275.
- (82) This temperature shift is used just to show that the temperature dependences of  $t$  and  $t^*$  are very similar. The division by a constant factor would show the same result.
- (83) Fragiadakis, D.; Casalini, R.; Bogoslovov, R. B.; Robertson, C. G.; Roland, C. M. Dynamic Heterogeneity and Density Scaling in 1,4-Polyisoprene. *Macromolecules* **2011**, *44*, 1149–1155.
- (84) Donth, E. The Size of Cooperatively Rearranging Regions at the Glass Transition. *J. Non-Cryst. Solids* **1982**, *53*, 325–330.
- (85) Donth, E. *The Glass Transition*; Springer-Verlag: Berlin, 2001.
- (86) Berthier, L.; Biroli, G.; Bouchaud, J. P.; Cipelletti, L.; El Masri, D.; L'Hôte, D.; Ladieu, F.; Pierno, M. Direct Experimental Evidence of a Growing Length Scale Accompanying the Glass Transition. *Science* **2005**, *310*, 1797–1800.
- (87) Berthier, L.; Biroli, G.; Bouchaud, J. P.; Kob, W.; Miyazaki, K.; Reichman, D. R. Spontaneous and Induced Dynamic Fluctuations in Glass Formers. I. General Results and Dependence on Ensemble and Dynamics. *J. Chem. Phys.* **2007**, *126*, 184503.
- (88) Capaccioli, S.; Ruocco, G.; Zamponi, F. Dynamically Correlated Regions and Configurational Entropy in Supercooled Liquids. *J. Phys. Chem. B* **2008**, *112*, 10652–10658.
- (89) Hao, S. G.; Wang, C. Z.; Li, M. Z.; Napolitano, R. E.; Ho, K. M. Dynamic Arrest and Glass Formation Induced by Self-aggregation of Icosahedral Clusters in  $\text{Zr}_{1-x}\text{Cu}_x$  Alloys. *Phys. Rev. B* **2011**, *84*, 064203.
- (90) Ngai, K. L.; Capaccioli, S. Relation Between the Activation Energy of the Johari–Goldstein  $\beta$  Relaxation and  $T_g$  of Glass Formers. *Phys. Rev. E* **2004**, *69*, 031501.